J Mater Sci (2009) 44:4789–4795
DOI 10.1007/s10853-009-3721-3

Processing and properties of poly(ε-caprolactone)/carbon nanofibre composite mats and films obtained by electrospinning and solvent casting

Ilaria Armentano · Costantino Del Gaudio · Alessandra Bianco · Mariaserena Dottori · Francesca Nanni · Elena Fortunati · Josè Maria Kenny

Received: 29 May 2009 / Accepted: 2 July 2009 / Published online: 22 July 2009

Abstract Composite materials based on poly(ε-caprolactone) (PCL) and carbon nanofibres (CNFs) were processed by solvent casting and electrospinning. The main objective was to investigate the effects of the CNFs on the microstructural, thermal and mechanical properties of the PCL matrix composites processed by two different routes. The hybrid materials obtained with different CNF content (1, 3 and 7 wt%) were analysed by electron microscopy (FESEM), differential scanning calorimeter (DSC), thermogravimetry (TGA) and mechanical testing. The composite films showed a good dispersion in the PCL matrix while electrospun samples were consisted of homogeneous and uniform fibres up to 3 wt% CNFs with average fibre diameter ranged between 0.5 and 1 μm. Composite films and mats revealed an increased crystallization temperature with respect to the neat PCL matrix. Mechanical properties of solvent cast films and electrospun mats were assessed by uniaxial tensile tests. A stiffness increase was achieved in PCL films depending on the CNF content, while mechanical properties of mats were only slightly affected by CNF introduction.

I. Armentano (✉) · E. Fortunati · J. M. Kenny
Material Science and Technology Center, UdR INSTM, NIPLAB, University of Perugia, Terni, Italy
e-mail: Ilaria.armentano@lnl.infn.it

C. Del Gaudio · A. Bianco · F. Nanni
Department of Chemical Sciences and Technologies, Research Unit INSTM Tor Vergata, University of Rome "Tor Vergata", Rome, Italy

M. Dottori
I.N.B.B. at Material Science and Technology Center, University of Perugia, Terni, Italy

Introduction

Poly(ε-caprolactone) (PCL) is a semicrystalline bioresorbable poly(α-hydroxyester), having an orthorhombic crystal structure [1, 2]. Due to its hydrophobic nature and high crystallinity degree, PCL degrades slowly [1, 3] by hydrolysis and has been considered in a wide range of possible applications, such as biodegradable packaging materials [4], implantable biomaterials, scaffold and microparticles for drug delivery [5, 6].

Carbon nanofibres (CNFs) are cylindrical or conical structures with diameters varying from a few to hundreds of nanometers and lengths ranging from less than a micron to millimeters. The internal structure of carbon nanofibres consisted of different arrangements of modified graphene sheets ordered [7]. Excellent electrical conductivity and mechanic-chemical properties characterise CNFs, as suitable candidates for polymer nanohybrid materials, since the nanosized diameter (i.e. 70–200 nm) provides high specific areas with enormous potential to modify the polymer matrix properties and, in particular, to improve the electrical conductivity and the mechanical properties [8].

In the last two decades, there has been a continuous increase of research for the improvement of material properties employing nanometric engineered structures taking advantage of the inherent high surface area–volume ratio of nanomaterials. In recent years, polymer nanohybrids have become a great challenge for scientists in order to create novel polymer-based systems with peculiar structural and functional properties [7].

Solvent casting represents a flexible, low-cost and short-term process widely used for the fabrication of nanohybrid polymer based films. On the other hand, electrospinning is a straightforward technique to produce non-woven micro- or nanofibrous mats, based on the application of high voltage

to a polymeric solution, in order to create an electrically charged jet randomly collected onto a grounded target [9]. Recently, the electrospinning technique has also been used for carbon nanostructures alignment in a polymer matrix and it has been reported that high aspect-ratio CNFs can orientate along the axis of electrospun fibres due to the sink flow and the high extension of the electrospun jet [10]. The carbon nanofibre alignment, however, depends upon the CNF dispersion in the polymer solution [11]. The idea of dispersing and aligning carbon nanostructures in polymer matrix to form highly ordered structures and composite materials has significant technological implications [12]. Hence, nanohybrid polymeric mats are being considered for use in composite materials, sensors, filtration, catalysis, protective clothing, biomedical applications (including wound dressing and scaffolds for tissue engineering, implants and membranes), space applications such as solar sails, and micro- and nano-optoelectronics (nanowires, LEDs, photocells, etc.) [13, 14].

In the present study, PCL films and electrospun mats loaded with CNFs were prepared by solvent casting and electrospinning technique and the effects of CNF concentration (1, 3, 7 wt%) on the properties of the composite materials were analysed. Nanocomposite microstructure and thermal behaviour were investigated by scanning electron microscopy (FESEM), differential scanning calorimeter (DSC) and thermogravimetry (TGA). Mechanical properties were evaluated by tensile tests.

Experimental part

Materials

Poly(ε-caprolactone) (PCL, M_n=80000) was supplied by Sigma-Aldrich. Tetrahydrofuran (THF), *N*,*N* dimethylformamide (DMF) and chloroform ($CHCl_3$) were supplied by Carlo Erba Reagenti.

Carbon iron free graphitized nanofibres (Pyrograf® HHT Grade) were used (specific surface area 25 m^2/g, Fe content lower than 400 ppm). CNFs were characterised morphologically and thermally by field emission electron microscopy (FESEM, Supra 25-Zeiss, Germany) and by thermogravimetry (TGA) using a quartz rod microbalance (Seiko Exstar 6000, Cheshire, UK). TGA was performed in air flow (50 mL min^{-1}) from 30 to 1000 °C with a 5 °C min^{-1} heating ramp.

Preparation of PCL/CNFs films

Neat and composite PCL films were obtained by solvent casting. In the first case, PCL granules were added to $CHCl_3$, the mixture was magnetically stirred at room temperature (RT) after it was completely dissolved. Thereafter, the polymeric solution was cast on a teflon support, air dried for 48 h at RT and for further 48 h in vacuum. The neat PCL solvent cast film was designated as PCLf.

In order to obtain nanohybrid films, CNFs were previously debundled in $CHCl_3$ by means of ultrasonication treatment (Ultrasonic bath-mod.AC-5, EMMEGI) for 4 h. PCL was added to suspension and magnetically stirred until the polymer dissolution was completed. The nanohybrid mixture was cast on to teflon substrate and air dried for 48 h at RT and for further 48 h in vacuum. Nanocomposite films of 10 cm in diameter and 300 μm thick, containing 1, 3 or 7 wt% CNFs, were obtained. Resulting samples were designated as PCL1f, PCL3f and PCL7f, respectively.

Preparation of electrospun PCL/CNFs mats

Nanohybrid PCL/CNFs mats of different composition (i.e. 1, 3 and 7 wt%) were produced by means of electrospinning technique following a two-step procedure.

The selected amount of carbon nanostructure was dispersed in a mixture of THF:DMF (1:1) and ultrasonicated for 1 h. Then, PCL was added (14% w/v) and the resulting suspension magnetically stirred at room temperature until polymer dissolution was completed. The mixture was poured into a glass syringe fitted with a metallic blunt tip needle (22G), connected to the positive output of a high voltage power supply, set at 12 kV (Spellman, USA). A controlled flow was achieved by means of a syringe pump, running at 0.4 mL/h (KD Scientific, USA). Electrospun mats were collected in air at RT on to an aluminium target (ϕ 10 cm) fixed at 15 cm from the tip of the needle. As-spun samples were then vacuum dried for 48 h. The resulting electrospun composites were designated as PCL1m, PCL3m and PCL7m, respectively. The neat PCL electrospun mat was designated with PCLm.

Microstructural, thermal and mechanical characterisation

FESEM (Supra 25-Zeiss, Germany) was used to study the morphology of the PCL/CNFs nanohybrid films and electrospun mats. Cross-sections obtained by sample fracture in liquid nitrogen and top views were observed. The average electrospun fibre diameter was computed from FESEM micrographs, considering around 50 fibres randomly selected.

Thermal properties were assessed by differential scanning calorimetry (DSC 822/e Mettler-Toledo, USA) for all samples in the following conditions: heating rate 10 °C min^{-1}, temperature range from −25 to 100 °C.

Thermal cycles consisted in a heating ramp followed by a cooling ramp and a final heating ramp. Melting temperatures (T_{m1} and T_{m2}), enthalpies (ΔH_{m1} and ΔH_{m2}) and crystallinity degrees (χ_{m1} and χ_{m2}) were determined either from first and second heating scans. Crystallization temperature (T_c) and enthalpy (ΔH_c) were measured from the cooling cycle. The crystallization degree was calculated according to the following relation:

$$\chi = \frac{1}{(1 - m_f)}\left[\frac{\Delta H}{\Delta H_{m0}}\right] \quad (1)$$

where ΔH and ΔH_{m0} were the scan-related enthalpy and the melting enthalpy associated to 100% crystalline PCL, respectively, and m_f is the nominal CNF weight fraction. ΔH_{m0} value was assumed to be 136 J/g [15]. Thermogravimetric analyses (TGA) were performed using a quartz rod microbalance (Seiko Exstar 6000) in the following conditions: sample weight 10 mg, N_2 flow (250 mL min^{-1}), temperature range 30–900 °C, heating rate 10 °C min^{-1}.

The mechanical behaviour of solvent cast films and electrospun mats was evaluated by tensile test (Lloyd LR 30 K, TA-HDi Stable Micro Systems), on the basis of ASTM-D 882, as follows: cross-head speed 5 mm min^{-1}, sample size 50 × 10 mm^2, load cell 50 N. Five specimens were tested for each material. The tensile modulus (E) was calculated in the linear region of the stress–strain curve, as proposed by Vaz [16]. Tensile strength (σ_b) and strain at break (ε_b) were also determined.

Results and discussion

CNF microstructure and thermal degradation

The TGA thermogram and the FESEM micrograph (insert) of CNFs are shown in Fig. 1. CNF thermal degradation in air was monitored to analyse the CNF purity. The residual mass at 1000 °C was 0.6 wt%, normally associated to catalyst, while the time derivative weight loss curve (DTG) shows that the thermal degradation process occurs in a single weight loss step, confirming the high CNF purity grade. FESEM images (insert) showed individually separated cylindrical carbon fibres characterised by rough surface sidewalls, the diameters ranging between 100 and 200 nm. Moreover, some hollow CNFs were also detected within the sample.

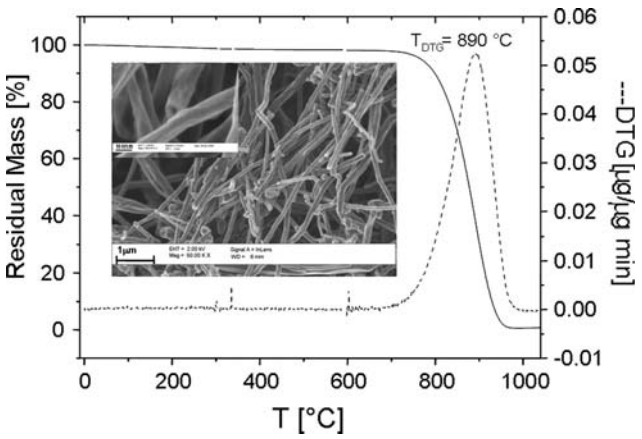

Fig. 1 Thermogravimetric analysis and FESEM micrograph (insert) of carbon nanofibres

Microstructure of PCL/CNFs nanocomposites

FESEM micrographs of the cross-section of samples PCL1f and PCL7f are reported in Fig. 2a, b and c, d, respectively. The polymeric matrix wraps itself around randomly distributed CNFs. In particular, at high content (i.e. 7 wt%), CNFs are uniformly dispersed in the matrix and a regular CNF distribution is revealed.

FESEM micrographs of PCL/CNFs mats fabricated by electrospinning are shown in Fig. 3. All electrospun fabrics showed a well-defined non-woven fibrous architecture. Up to CNF 3 wt%, samples were consisted of homogeneous and uniform fibres, as shown in Fig. 3a, c. Only in the PCL7m some defects were detected. This microstructure is ascribed to poor CNF dispersion, induced by increasing nanofibre interactions and entanglements (Fig. 3d). An efficient CNF dispersion is a crucial feature in reducing physical interactions among fibres and develops a strong interface between the carbon nanostructure and the polymeric matrix.

The calculated average fibre diameter was 0.8 ± 0.3 μm for the neat PCL electrospun mat. The mean diameter of nanohybrid fibres was 0.6 ± 0.3, 1.1 ± 0.5 and 1.2 ± 0.6 μm for samples PCL1m, PCL3m and PCL7m, respectively. The proximity of the values and the dispersion of these measurements do not allow any conclusive consideration on the effects of the CNF content on fibres diameter. However, there is a clear difference between the diameter of composite fibres (i.e. PCL1m) with respect to the pure matrix (PCLm). The reduction of the diameter of the composites can be ascribed to the increased electrical conductivity of the suspension to be spun. Higher nanofibres contents can induce an ineffective preliminary nanofibre dispersion and an increased packing density in the composite fibre inducing the formation of microdefects in the mat (i.e. PCL7m).

Finally, the effects of different solvents used for the realisation of films and mats need to be elucidated. Solvent cast films and electrospun mats were processed starting from solutions using $CHCl_3$ as solvent. In this case, the resulting morphology was remarkably heterogeneous, showing large fibres surrounded by a web-like structure of smaller ones (data not shown). This effect can be related to specific properties of $CHCl_3$ (i.e. electron-pair donicity,

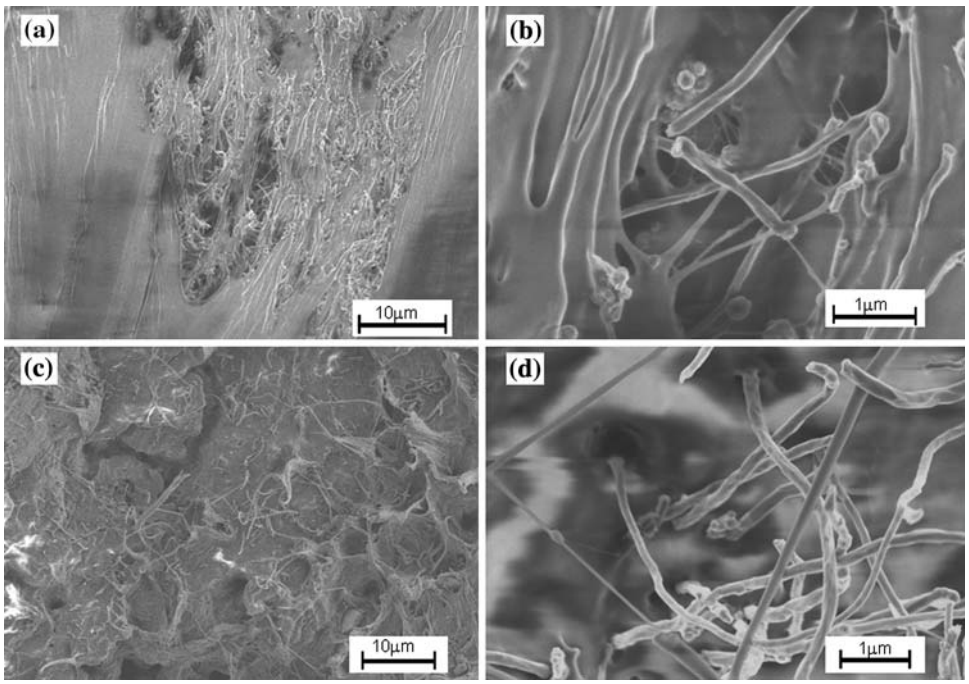

Fig. 2 FESEM micrographs of solvent cast PCL/CNFs films (cross-sections) loaded with different amounts of carbon nanofibres **a**, **b** CNFs 1 wt% and **c**, **d** CNFs 7 wt%, at different magnification

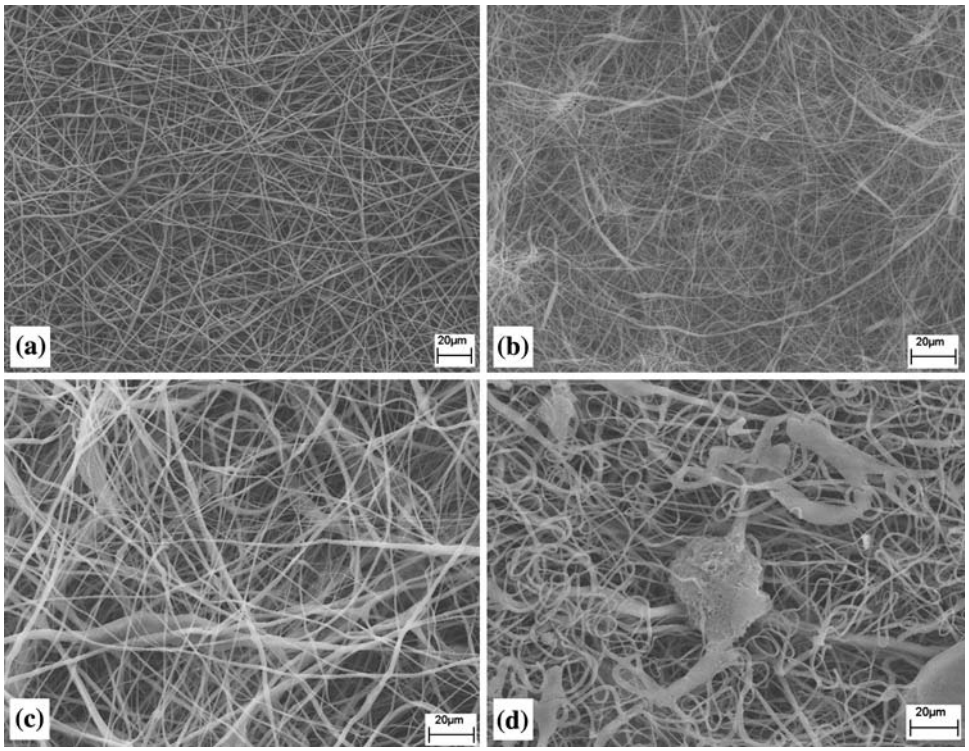

Fig. 3 SEM micrographs of **a** neat PCL electrospun mat and PCL/CNFs electrospun mats loaded with different amounts of carbon nanofiller **b** CNFs 1 wt%, **c** CNFs 3 wt%, **d** CNFs 7 wt%

solvochromic parameter, hydrogen bond donation parameter and dielectric constant) that can prevent an effective dispersion of carbon nanostructures compared to DMF [17]. In this respect, the collection of nanohybrids electrospun fibres was properly achieved using an opportune solvent mixture THF:DMF (1:1).

Thermal analysis of PCL/CNFs nanocomposites

Thermal analysis is a useful instrument to analyse structure–property correlations in polymer nanocomposites. Therefore, DSC measurements were performed on solvent cast films and electrospun mats. First heating and cooling

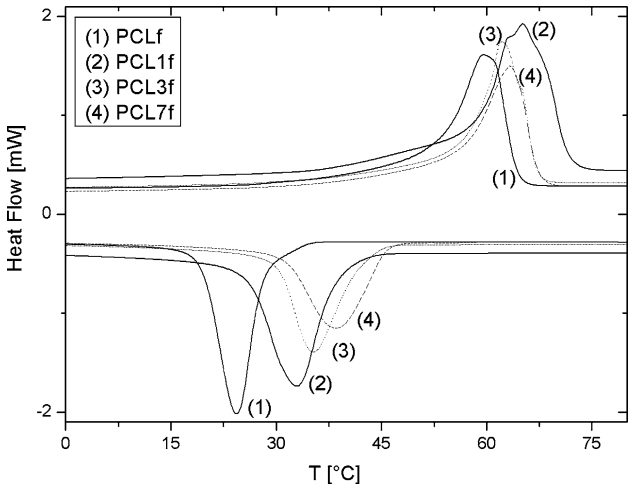

Fig. 4 Differential calorimetry curves of PCL/CNFs solvent cast films containing different carbon nanofibre amount

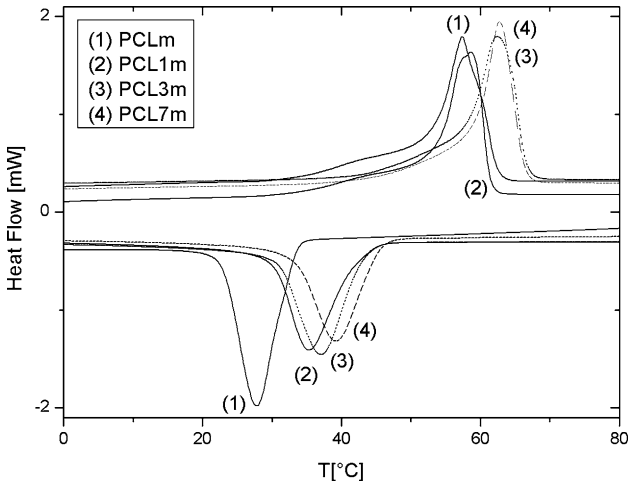

Fig. 5 Differential calorimetry curves of PCL/CNFs electrospun mats containing different carbon nanofibre amount

scans of solvent cast films and electrospun membranes at different composition are shown in Figs. 4 and 5, respectively. The thermal properties obtained from the thermograms are reported in Table 1. It can be observed that in solvent cast films, the nanocomposite melting temperature is shifted upwards (i.e. for PCL1f, T_{m1} is 4 °C higher than in neat PCL). This result indicates the development of a PCL/CNFs interface in which the polymer reorganizes itself with improved order and crystal dimensions (Fig. 4). Moreover, nanocomposites show a shoulder in the melting curve that revealed the presence of a crystalline fraction characterised by intermediate properties between bulk PCL and enhanced PCL/CNFs interface crystals. Furthermore, T_c progressively increased with the CNF content, revealing that CNFs are able to promote PCL crystallization by heterogeneous nucleation. These general results are coherent with a homogeneous dispersion of CNFs within the PCL matrix and a good affinity between the polymer and nanofibre sidewalls within the compositional values investigated. The enhanced crystal nucleation, due to the CNF presence, reduces the polymer chain bulk ability to be fully incorporated into growing crystalline lamella [18] leading to the formation less ordered polymer crystals characterised by more defected crystalline lamella. As a result of this bulk effect, all nanohybrid samples showed χ_{m1} and χ_{m2} values lower (or at least comparable) than neat PCL as in the case of PCL7f (Table 1).

In electrospun mats (Fig. 5), the CNF introduction induces a pronounced T_c shift, with increments as high as 10 °C for PCL7m respect to PCLm indicating a higher crystallization kinetic effects probably as a consequence of a higher ordered hybrid system. However, solvent cast films and electrospun membranes showed the same trend in T_m and consequently a similar development of the PCL/CNFs interface within fibres. Table 1 results show that electrospun mats are characterised by lower melting enthalpy and consequently lower crystallinity degree respect to solvent cast films. Regarding the effects of the CNFs added, it can be noticed that nanohybrid mats show improved crystallinity degrees with respect to the pure matrix. Moreover, during the cooling scan, CNFs produce

Table 1 Thermal properties of PCL and PCL/CNFs solvent cast films and electrospun mats

Sample	T_{m1} (°C)	T_c (°C)	ΔH_{m1} (J/g)	χ_{m1}[a] (%)	ΔH_c (J/g)	T_{m2} (°C)	ΔH_{m2} (J/g)	χ_{m2}[a] (%)	T_{m1} (°C)
PCLf	60.4 ± 0.9	24.5 ± 0.2	86 ± 1	63.0 ± 0.2	68.4 ± 0.3	56.5 ± 0.7	68.2 ± 0.2	50.2 ± 0.2	60.4 ± 0.9
PCL1f	64 ± 2	34 ± 2	87 ± 2	65 ± 1	59 ± 2	57.0 ± 0.7	66 ± 1	49 ± 1	64 ± 2
PCL3f	62.7 ± 0.9	35.3 ± 0.2	83 ± 2	62.8 ± 0.2	59.1 ± 0.2	57.6 ± 0.2	67 ± 2	50.3 ± 0.3	62.7 ± 0.9
PCL7f	62.8 ± 0.5	38.4 ± 0.2	77 ± 3	61 ± 1	56 ± 1	57.1 ± 0.2	65 ± 2	52 ± 2	62.8 ± 0.5
PCLm	59.0 ± 0.9	28.5 ± 0.7	76.1 ± 0.7	56.3 ± 0.5	60 ± 2	56.4 ± 0.2	67 ± 1	49.2 ± 0.7	59 ± 0.9
PCL1m	58.9 ± 0.3	29.9 ± 0.2	78 ± 2	59 ± 1	62 ± 2	59 ± 2	68 ± 2	51 ± 2	58.9 ± 0.3
PCL3m	62.7 ± 0.5	36.6 ± 0.9	79.1 ± 0.9	60.2 ± 0.7	60 ± 2	59 ± 3	69 ± 2	52.4 ± 0.9	62.7 ± 0.5
PCL7m	62.5 ± 0.3	38.9 ± 0.2	74 ± 1	58.6 ± 0.9	57 ± 1	59 ± 2	66 ± 2	53 ± 1	62.5 ± 0.3

m melting, *c* crystallization

[a] $\chi = \Delta H_m/[(1-m_f) \cdot \Delta H_{m0}]$; ΔH_m (J/g) is the melting heat during respective scan, $\Delta H_{m0} = 136$ J/g [15]

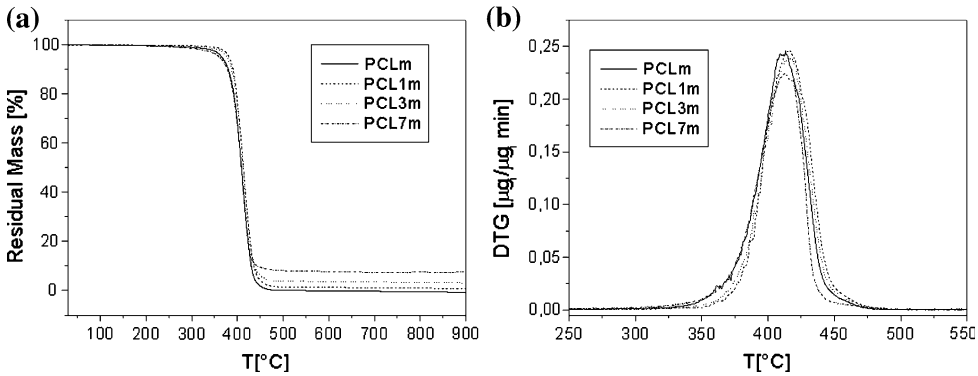

Fig. 6 TG (**a**) and DTG (**b**) curves of neat PCL and PCL/CNFs electrospun mats of different composition

heterogeneous nucleation, confirmed by T_c increase in all hybrid compositions.

Thermogravimetric analysis evidenced that PCL/CNFs solvent cast films and electrospun mats showed comparable thermal degradation. As an example, the TG and DTG curves of PCL/CNFs electrospun mats containing different carbon nanofibre amounts are shown in Fig. 6. The DTG curve of the neat PCL membrane reported in Fig. 6b showed one main loss at 414 °C, associated to polymer thermal degradation. A similar behaviour was detected for PCL1m, PCL3m and PCL7m mats, indicating that the polymer thermal degradation kinetic was not affected by the carbon nanofibre presence, since they are not covalently linked to the polymer matrix. As expected, a progressive increase of the residual mass with CNF content in the composite was detected (Fig. 6a).

Mechanical properties of PCL/CNFs nanocomposites

The tensile stress–strain curves of PCL/CNFs films are reported in Fig. 7 while the mechanical properties measured are reported in Figs. 8 and 9. The addition of few CNF weight percentage resulted in a strong reinforcing

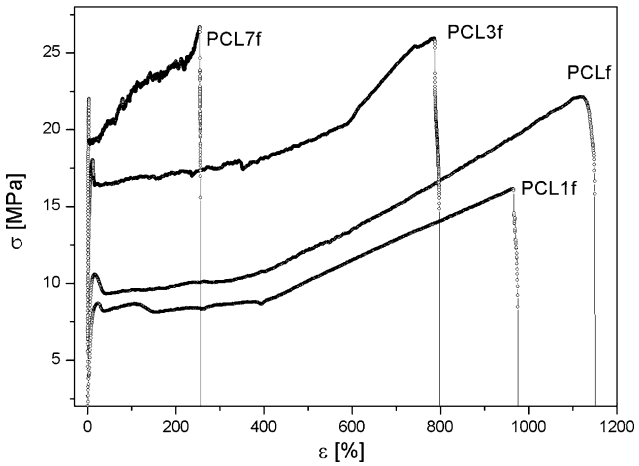

Fig. 7 Tensile stress–strain curves of PCL/CNFs films

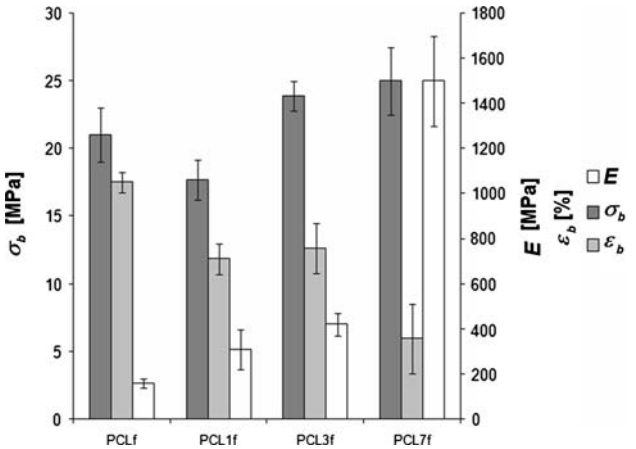

Fig. 8 Tensile mechanical properties of PCL/CNFs solvent cast films

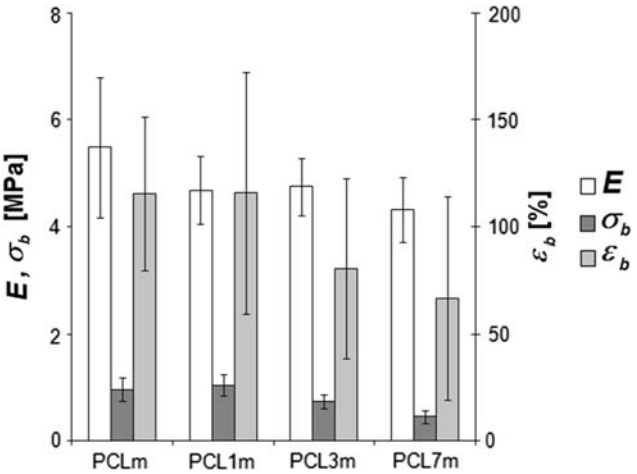

Fig. 9 Tensile mechanical properties of PCL/CNFs electrospun mats

effect, raising up the tensile modulus and inhibiting polymer drawing. The increase of the nanohybrid tensile modulus proceeds linearly with the CNF content. Nanocomposite mechanical properties depend on the strength of interface that relays on the interaction between the polymeric matrix and the nanostructure. In CNF reinforced films CNFs inhibit the macromolecular sliding of chains.

Tensile strength (σ_b) of PCL decreased from 21 to 17 MPa in PCL1f and this effect can be ascribed to drawing inhibition, while σ_b was improved for PCL3f and PCL7f specimens. A remarkable reinforcement effect, predominant on drawing inhibition, was observed in PCL7f, since tensile strength increased 14% with respect to the final strength of the neat matrix but was increased by 150% for the same level of deformation with only 7 wt% of CNFs. Moreover, the tensile modulus increased one order of magnitude respect to neat PCLf, resulting 1.4 GPa. Mechanical properties revealed that incorporation of high aspect ratio CNFs into the PCL matrix significantly enhanced the polymer stiffness [19].

PCL/CNFs electrospun mats showed that the addition of CNFs was not effective in increasing the mechanical properties (Fig. 9). However, the elongation at break and the tensile strength showed a decreasing trend that can be associated to the presence of micrometric agglomerates, especially in the case of PCL7m, as confirmed by FESEM (Fig. 3d). Average tensile modulus was in the range 5.4–4.3 MPa, tensile strength 1.0–0.4 MPa, strain at break 115–66%, starting from PCLm to PCL7m. The entanglements between polymer fibres and the CNF alignment within polymeric fibre axis affect mechanical properties in fibrous mats [20–22]. The increase of carbon nanofibre content limits this effect and promotes CNF agglomerates acting as stress concentration points, weakening the structure [18].

Conclusions

PCL/CNFs composites were obtained by solvent casting and electrospinning. Morphological, thermal and mechanical properties of PCL/CNFs nanohybrids were investigated as a function of CNF content. In solvent cast composite films, the CNF presence in the polymer matrix resulted in increased crystallization temperature and in mechanical reinforcement, with the reduction of the elongation at break and with a remarkable improvement of the elastic modulus. Similarly, in electrospun composite mats the PCL crystallization temperature increased while mat mechanical properties were not significantly affected by the presence of fibres. In conclusion, the assessed modulation of PCL matrix composites obtained by adding selected carbon nanofibre amounts opens new challenges in the field of functional hybrid systems.

Acknowledgements The authors are grateful to the Italian Interuniversity Consortium on Materials Science and Technology (INSTM) for the financial support (PRISMA 2007—Studio dell'orientamento e dei fenomeni di segregazione indotti in matrici polimeriche ibride ed in miscele polimeriche elettrofilate). M. Dottori acknowledges the INBB Institute for the financial support.

References

1. Ciardelli G, Chiono V, Vozzi G, Pracella M, Ahluwalia A, Barbani N, Cristallini C, Giusti P (2005) Biomacromlecules 6:1961
2. Lovinger AJ, Han BJ, Padden FJ Jr, Mirau PA (1993) J Polym Sci Part B: Polym Phys 31:115
3. Martin DP, Williams SF (2003) Biochem Eng J 16:97
4. Messersmith PB, Giannelis EP (1995) J Polym Sci A 33:1047
5. Pektok E, Nottelet B, Tille JC, Gurny R, Kalangos A, Moeller M, Walpoth BH (2008) Circulation 118:2563
6. Aishwarya S, Mahalakshmi S, Sehgal PK (2008) J Microencapsul 25:298
7. Dresselhaus MS, Dresselhaus G, Eklund PC (2001) Science of Fullerenes and Carbon nanotubes. Academic Press, San Diego
8. Sandler J, Werner P, Shaffer M, Demchuk V, Alstadt V, Windle AH (2002) Composites Part A 33:1033
9. Frenot A, Chronakis IS (2003) Curr Opin Colloid Interface Sci 8:64
10. Ago H, Tobita M (2002) Adv Mater 14:1380
11. Xie XL, Mai YW, Zhou XP (2005) Mater Sci Eng R 49:89
12. Saeed K, Park SY, Lee HJ, Baek JB, Huh WS (2006) Polymer 47:8019
13. Li D, Xia Y (2004) Adv Mater 16:1151
14. Jayaraman K, Kotaki M, Zhang Y, Mo X, Ramakrishna S (2004) J Nanosci Nanotechnol 4:52
15. Guo Q, Harrats C, Groeninckx G, Reynaers H, Koch MHJ (2001) Polymer 42:6031
16. Vaz C, van Tuijl S, Bouten CVC, Baaijens FPT (2005) Acta Biomaterialia 1:575
17. Torrens F (2006) Int J Quantum Chem 106:712
18. Wu D, Wu L, Sun Y, Zhang M (2007) J Polym Sci Part B: Polym Phys 25:3137
19. Marras SI, Kladi KP, Tsivintzelis I, Zuburtikudis I, Panayiotou C (2008) Acta Biomater 4:756
20. Ko F, Gogotsi Y, Ali A, Naguib N, Ye H, Yang G, Li C, Willis P (2003) Adv Mater 15:1161
21. Dror Y, Salaha W, Khalfin RL, Cohen Y, Yarin AL, Zussman E (2003) Langmuir 19(17):7012
22. Li L, Bellan LM, Craighead HG, Frey MW (2006) Polymer 47:6208